

# Long-term X-ray Variability and the Importance of the ASM

S.D. Vrtilik

*Harvard-Smithsonian Center for Astrophysics, 60 Garden Street, Cambridge, MA 02138 USA*

**Abstract.** From determining the  $\log(N)$ - $\log(S)$  distribution of XRBs in the Milky Way, to testing radio/X-ray correlations of microquasars and BHCs, studying long term variability, and acting as a trigger for observations of transient sources, the ASM on RXTE has proved an invaluable resource. I will briefly discuss some highlights of the many results that have been possible only because of the ASM. The fact that the number of papers per year (over 100) that have relied on ASM data has remained steady over the 8-year lifetime of the RXTE is an indication of the enduring usefulness of all-sky X-ray monitoring. I argue that the permanent presence in space of an ASM-like instrument is a major benefit to numerous active branches of astrophysics, that there is no substitute (ground-based or in other parts of the electromagnetic spectrum) for this capability, and that the planning process for future missions ought to take into account the ongoing scientific need for all-sky X-ray monitoring.

## INTRODUCTION

The All-Sky Monitor (ASM) on RXTE consists of three wide-angle shadow cameras equipped with proportional counters with a total collecting area of  $90 \text{ cm}^2$  (Levine *et al.* 1996). It observes continuously covering 80% of the sky every 90 minutes with a spatial resolution of  $3' \times 15'$ . Timing and spectral information (1.2 to 12.1 keV divided into three energy channels) are provided to within a thousandth of a day.

The NASA Astrophysics Data System shows a steady stream of papers (over 100 per year in refereed journals: Hale Bradt, personal communication) with high citation rates that have relied on data from the ASM. In this paper we highlight some examples of science that utilized the RXTE/ASM. Topics range from determinations of long-term periods, and  $\log(N)$ - $\log(S)$  for X-ray binaries, to studies on star formation and state transitions, correlated multiwavelength studies, and the many works that relied on triggers from the RXTE. Based on these examples I make an appeal for the continued presence of X-ray ASMs.

## LONG-TERM VARIABILITY

Studies of periodicities in the lightcurves of persistent X-ray binaries provide us with information on the physical mechanisms that drive the variability. Long-term variability studies are only possible when systematic observations are available over a time period considerably longer than the variability. Clarkson *et al.* (2003b) used 6.1 years of ASM data to search for a long-term period

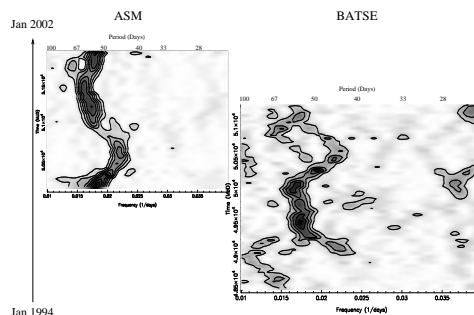


**FIGURE 1.** Dynamic power spectrum for the 20-100 keV lightcurve of SMC X-1 observed by BATSE over 9 years (right) and for the 1.3-12.1 keV lightcurve provided by RXTE over 6 years (left). From Clarkson *et al.* (2003b).

in the massive X-ray binary SMC X-1. SMC X-1 has a known orbital period of 3.9 days and a pulse period of 0.7 seconds. Earlier studies using shorter segments of ASM data (Levine *et al.* 1996; Wojdowski *et al.* 1998) first noted the presence of a superorbital period that was not steady but varied between 50-60 days. Clarkson *et al.* conducted a dynamic power spectrum (DPS) analysis designed to follow closely all changes in the X-ray modulation. In Figure 1 the period range (50-60 days) is clear and in addition it can be seen that the range itself varies over a timescale of 7 years. A key point to note is the close correlation found between the RXTE/ASM and CGRO/BATSE results. These are two instruments with different orbital precession periods, working on completely different principles, and covering a large range

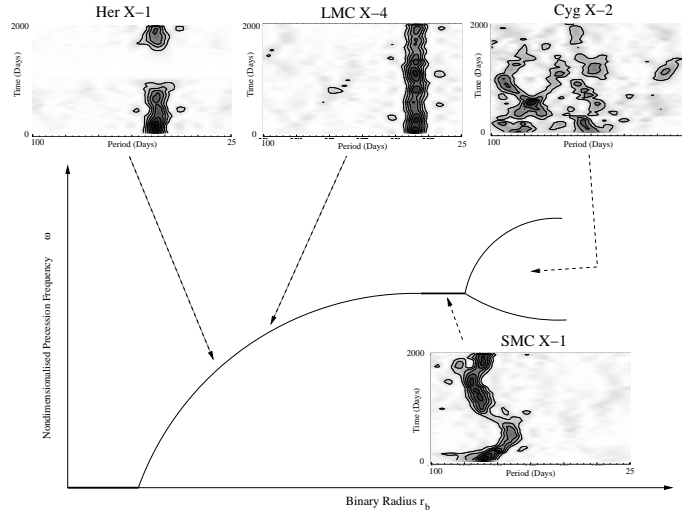


**FIGURE 2.** Schematic bifurcation diagram for radiation-driven warping. As the control parameter  $r_b$  is increased, the number of stable precession solutions increases. Initially there are none, then stable mode-0 precession rising in frequency as  $r_b$  increases (solid line). Near the mode region border, the solution becomes marginally unstable as short-lived mode-1 instabilities form (thick line). Finally in the mode 1+ region, two or more steady solutions are possible, and the system precesses at a combination of these warping modes. From Clarkson *et al.* (20003a).

in energy. Clarkson *et al.* were able to identify the soft component of the ASM lightcurve with the accretion disk or matter expelled from the stellar companion whereas the hard component was found to be associated with the emission at or near the surface of the neutron star. This study allowed for the elimination of several mechanisms proposed to explain the superorbital period (For example, varying absorption is ruled out since the hard X-ray BATSE lightcurve behaves in the same way as the ASM lightcurve) and showed that the superorbital variation of SMC X-1 is fully consistent with current stability theories of warps in accretion disks.

Clarkson *et al.* (2003a) expanded their longitudinal study of SMC X-1 into a synoptic study of several X-ray binaries. Of these the superorbital periods of Cyg X-2 and SMC X-1 were first detected by the ASM (Levine *et al.* 1996). These seemingly different systems turn out to be compatible with a radiation induced warping mechanism. This mechanism, introduced by Wijers & Pringle (1999) and others in the mid-90s and based on early work by Katz (1973) and others, was worked out in some detail by Ogilvie and Dubus in 2001. As the binary separation is increased the number of stable precession solutions increases; at one point the solution becomes unstable and following that point two or more steady solutions are possible and the system precesses at a combination of these warping modes (Figure 2). When the positions of the sources Her X-1, LMC X-4, SMC X-1, and Cyg X-2 (as determined by their binary separation) are placed on the model, their behavior is fully commensurate with their system parameters as shown in

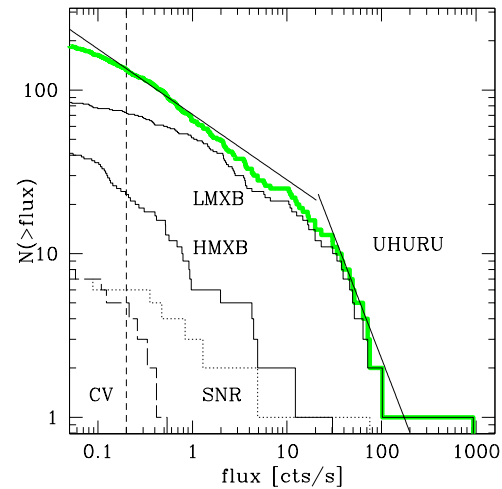


**FIGURE 3.** Number-flux relation for all galactic sources derived from the entire ASM sample. The broken solid line shows schematically the number-flux relation for the low-latitude  $|b| < 20^\circ$  sources obtained by Uhuru (Matilsky *et al.* 1973). The vertical dashed line shows approximate completeness limit of the ASM sample. The thick grey histogram shows the  $\log(N)$ - $\log(S)$  for all Galactic sources observed by ASM. The four lower histograms show the contributions of different classes of sources to the total galactic. from Grimm, Gilfanov, & Sunyaev 2002)

the DPS. Since separation is connected to orbital period, our early conclusion that the longer the orbital period the greater the uncertainty in superorbital period is supported

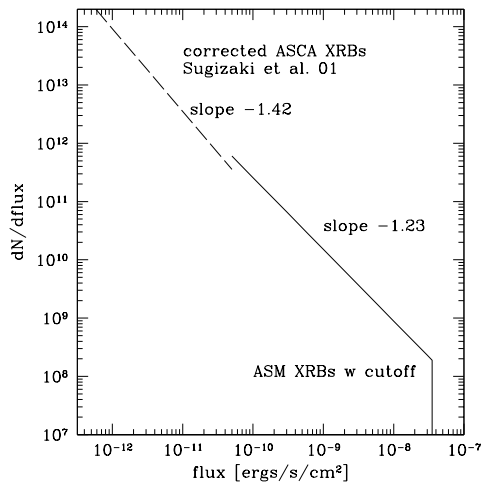


**FIGURE 4.** Comparison of the differential  $\log(N)$ - $\log(S)$  relation for Galactic X-ray binaries obtained by ASM (solid line with break) and by ASCA Galactic Ridge Survey (dashed line). The ASCA number-flux relation was multiplied by an approximate correction factor accounting for the difference in the sky coverage of the ASM and ASCA surveys. from Grimm, Gilfanov, & Sunyaev 2002)

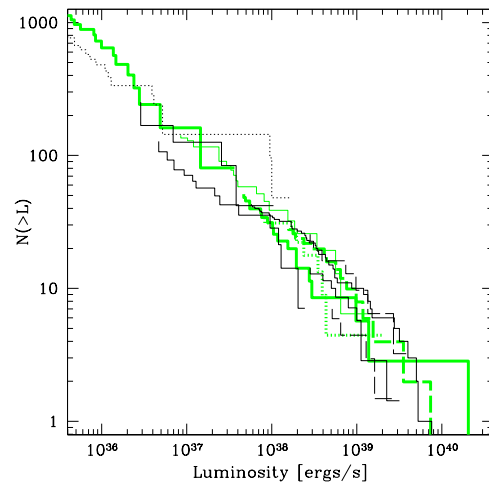


**FIGURE 6.** The luminosity functions for the same galaxies scaled by the ratio of their star formation rate to the SFR of the Antennae. The luminosity functions are plotted only above their corresponding completeness limit. From Grimm, Gilfanov, & Sunyaev (2003).

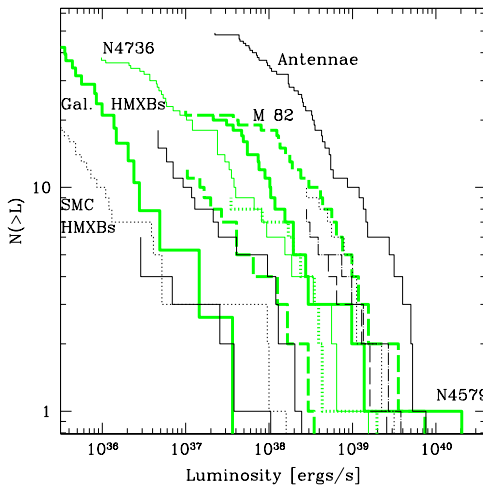


**FIGURE 5.** The luminosity functions of compact X-ray sources in nearby galaxies from the primary sample obtained by Chandra. From Grimm, Gilfanov, & Sunyaev (2003).

earlier studies they found significant differences in the spatial distribution of high and low mass XRBS, with HMXBs concentrated toward the Galactic plane and delineating the spiral structure while avoiding the Galactic bulge, and LMXBs favoring the Galactic bulge. Figure 3 shows the number flux relation for all galactic sources (to a limiting sensitivity of  $6.4 \times 10^{-11}$  ergs  $s^{-1}$   $cm^{-2}$ ) derived from the ASM. The  $\log(N)$ - $\log(S)$  for HMXBs is well described by a simple power law of slope 1.6 whereas the LMXBs have a slope of 1.2 and require a high-flux cutoff. A comparison of the differential  $\log(N)$ - $\log(S)$  relation for Galactic XRBS obtained by the ASM and by the ASCA Galactic Ridge Survey shows that although the ASCA GRS had 100 times better sensitivity it does not reveal any significant departures from the ASM result. The average LMXB luminosity function shows a break near the Eddington luminosity of a 1.4 solar mass neutron star; at least 16 XRBS observed by the ASM showed super-Eddington luminosity and the plotted distributions of these can be used to compare with Chandra and XMM images of nearby galaxies.

(Vrtilek *et al.* 2001).

## LOG(N)-LOG(S)

Recently, Grimm, Gilfanov, & Sunyaev (2002) constructed  $\log(N)$ - $\log(S)$  luminosity functions for XRBS using RXTE/ASM data. As expected from theory and

## STAR FORMATION

Using their studies of HMXB populations from the ASM, ASCA, and MIR-KVANT/TTM data and Chandra and ASCA observations of starburst galaxies Grimm *et al.* (2003) determined a linear relationship between HMXBs and star formation rates (SFR): namely that the luminosity distribution of HMXBs in a galaxy

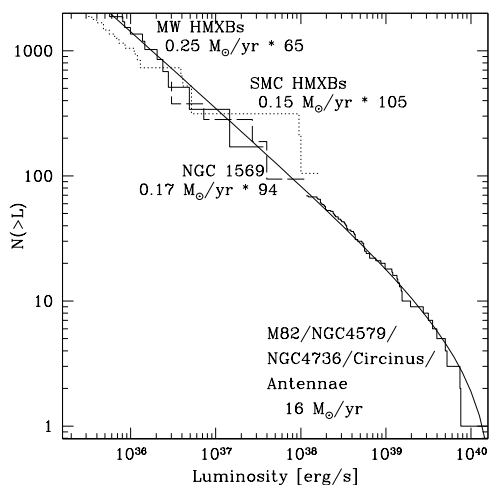


**FIGURE 7.** Combined luminosity function of compact X-ray sources in the starburst galaxies M82, NGC 4038/9, NGC 4579, NGC 4736 and Circinus with a total SFR of  $16 M_{\odot} \text{ yr}^{-1}$  (histogram above  $2 \cdot 10^{38} \text{ erg s}^{-1}$ ) and the luminosity functions of NGC 1569 and HMXBs in the Milky Way and Small Magellanic Clouds (three histograms below  $2 \cdot 10^{38} \text{ erg s}^{-1}$ ). The thin solid line is the best fit to the combined luminosity function of the starburst galaxies *only*. From Grimm, Gilfanov, & Sunyaev (2003).

can be described by an universal luminosity function whose normalization is proportional to the SFR and that the number of HMXBs is also related to the SFR. Figure 5 shows the luminosity function of XRBs from Chandra data. In Figure 6 all the LFs have been scaled to the SFR of the Antennae. Despite large differences (factors of 40-50) in SFRs the scaled LFs occupy a narrow band in N/ I-L phase.

A major surprise of this study is that in the low SFR regime the relation between SFR and collective luminosity of HMXBs is non-linear ( $L_X \sim \text{SFR}^{1.7}$ ) and becomes linear only for sufficiently high SFRs, when the total number of HMXB sources becomes sufficiently large.

Grimm *et al.* (2003) also demonstrated (based on Chandra observations of the HST Deep Field North) that the relationship between SFRs and the X-ray luminosity of HMXBs in a galaxy holds for distant star forming galaxies with redshifts as high as  $z=1.2$  (Figure 8). The good correlation between SFR and X-ray luminosity due to HMXBs provides a powerful and independent way to measure SFR in distant galaxies.

## MULTIWAVELENGTH STUDIES

In 2000, Chiang *et al.* used simultaneous observations with EUVE, ASCA, and RXTE to study the Seyfert 1

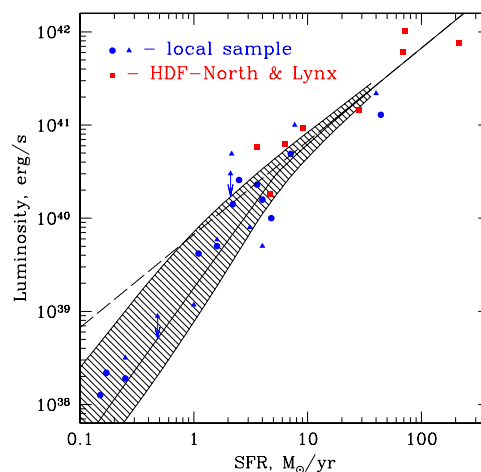


**FIGURE 8.** The  $L_X$ -SFR relation. The filled circles and triangles are nearby galaxies, the open circles are distant star forming galaxies from the HDF North and Lynx field. The arrows are the upper limits for the X-ray luminosity due to HMXBs for IC 342 and NGC 891. The thick solid line shows the expected relation between SFR and the most probable value of the total luminosity computed for the best fit parameters of the HMXB luminosity function. Note, that in the low SFR regime the probability to find a galaxy below the solid curve is  $\sim 10 - 15\%$ . The shaded area shows the 68% confidence region including both intrinsic variance of the  $L_X$ -SFR relation and uncertainty of the best fit parameters of the HMXB luminosity function. The dashed line shows the linear  $L_X$ -SFR relation. From Grimm, Gilfanov, & Sunyaev (2003).

galaxy NGC 5548. They found that variations in the EUV emission lead similar modulations at higher energies by 10-30 ks. This allowed the elimination of models in which the soft X-ray component is produced by re-processing of harder X-rays and implied that the variability of the optical through EUVE emission is the driver for variability in hard X-rays (perhaps through thermal Comptonization). They constructed a PDS from the ASM data which shows evidence for a break at a few times  $10^{-8} \text{ Hz}$ . The combined RXTE ASM/PCA power spectrum is remarkably similar to those from the low/hard states of Galactic black hole candidates such as Cygnus X-1. The implied scaling factor is comparable to the expected mass ratio for the two objects (Figure 9).

Correlated X-ray and radio studies of XRBs showed that radio jets are ubiquitous in sources with black holes or low magnetic fields. Choudhury *et al.* used ASM, BATSE, and 2.2 GHz radio data to study such Galactic microquasars. Figure 10 shows the low-hard states selected for this study using the ASM. Figure 11 shows the radio vs ASM flux in scatter diagrams for Cyg X-3, GRS 1915+05, and Cygnus X-1. Comparing these with published scatter diagrams for GX 339-4 and V404Cyg,

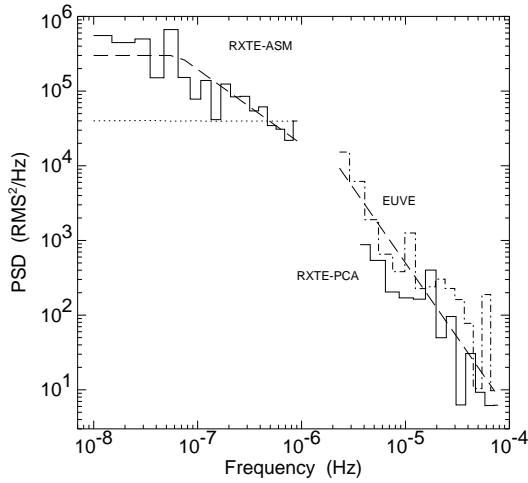


**FIGURE 9.** Power Spectral Densities constructed from RXTE-ASM, RXTE-PCA, and EUVE data. Dashed lines show flat,  $f^{-1}$ , and  $f^{-2}$  overlaid on the power spectra. The dotted line shows an estimate of the mean noise level of the ASM data. All PSDs are normalized such that integrating over positive Fourier frequencies yields the root mean square variability, normalized to the mean, for each particular light curve. From Chiang *et al.* 2000.

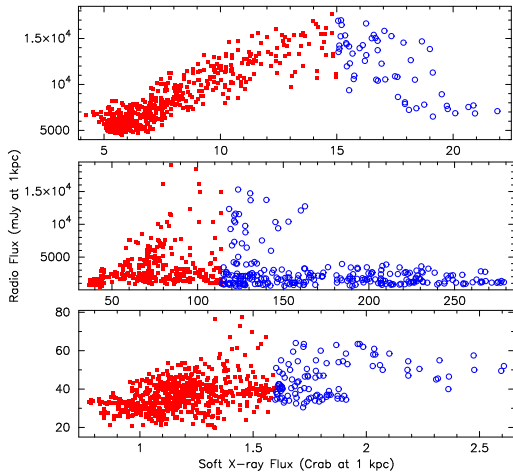


**FIGURE 10.** Radio (2.2 GHz) and soft X-ray (RXTE-ASM, 2-12 keV) emission scatter diagrams of Cyg X-3 (top panel), GRS 1915+105 (middle panel) and Cyg X-1 (bottom panel) for the long-term, steady, hard (filled squares) as well as soft (open circles) states, exclusive of data from the flaring states. From Choudhury, Rao, & Vadawale (2003).

they find that all the microquasars, although spanning 5 orders of magnitude in their intrinsic luminosities, show a monotonic increase of radio emission with soft X-ray emission and an anti-correlation with the hard X-rays detected by BATSE with a spectral pivoting around 20 keV that is correlated with the radio flux. Cyg X-3 de-

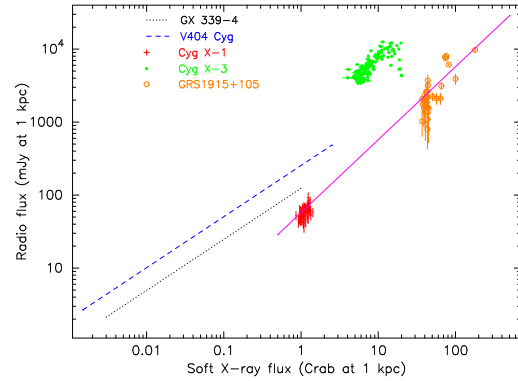


**FIGURE 11.** Radio (2.2 GHz) normalized to a distance of 1kpc against the soft X-ray (RXTE-ASM, 2-12 keV) normalized to Crab at 1 kpc for Cyg X-1, Cyg X-3, and GRS1915+105, in their low-hard states. The power-law fits (with an index of 0.7) reported for GX 339-4 and V404 Cyg by Gallo *et al.* (2002) are shown as dotted and dashed lines, respectively. The continuous line is a linear fit to the combined data of Cyg X-1 and GRS1915+105. From Choudhury, Rao, & Vadawale (2003).

viates from a single relation by an order of magnitude; this could be reconciled if the observed X-ray luminosity is an underestimate because of obscuration or the radio luminosity is an overestimate because of beaming. They qualitatively explain their findings with a two-component advective flow model where the location of the boundary layer between the thin disk and the comptonizing region determines the spectral shape and the amount of outflow. A complete understanding of the accretion-ejection physics of microquasars depends critically on such long-term multiwavelength studies.

Six years of optical AAVSO data combined with RXTE/ASM data of SS Cyg (one of the few cataclysmic variables detectable with the ASM) revealed that the 3-12 keV X-ray flux is suppressed during optical outbursts (McGowan, Priedhorsky, & Trudolyubov 2003). These results are in agreement with the modified disk instability models which invoke two-component accretion flow consisting of a cool optically thick accretion disk truncated at an inner radius and a quasi-spherical hot coronal flow extending to the surface of the white dwarf. McGowan *et al.* also found that the anomalous optical outbursts of SS Cyg are accompanied by short hard X-ray outbursts lasting 1-2 days. An all-sky monitor just a few times more sensitive than the RXTE/ASM would allow study of individual outbursts and quiescent states of SS Cyg with much greater signal to noise and extend such studies to a large number of dwarf novae (Priedhorsky, Peele, & Nugent 1996).

## STATE TRANSITIONS/TOO TRIGGERS

The highlights I have mentioned above do not include the numerous papers which resulted from observations made following a state transition in a system that triggered target-of-opportunity (TOO) observations. Undoubtedly one of the most significant contributions of the ASM was the provision of triggers for closer studies of unusual or unique events: Around 10% of Chandra and XMM observations are triggered by ASM monitoring. The breadth and depth of the science resulting from this ASM capability are well illustrated by other contributions to these proceedings as well as contributions to the meeting “XRBS in the Chandra and XMM-Newton era (with an emphasis on targets of opportunity)” organized by Miller and Garcia in 2002.

## SUMMARY

Due to its all-sky coverage and long operational time, the RXTE/ASM instrument is ideally suited for studying time-dependent properties of sources. It is also imperative for identifying specific states in order to trigger observations with other more specialized instruments. That the ASM has become an important resource for the community is reflected by the fact that ASM results are appearing in more than 100 papers a year in refereed journals and that ASM results are an ongoing important resource for about 10 observations, in addition to those of other satellites and ground based observatories.

The permanent presence in space of an ASM-like instrument is a major benefit to numerous active branches of astrophysics. Such an instrument can: provide rapid notification of new or state transitions; enable study of long-term lightcurves; facilitate longitudinal and correlative multiwavelength studies.

The rapid availability of ASM quick-look results to the entire community has done much to foster scientific productivity. There is no substitute (ground-based or in other parts of the electromagnetic spectrum) for this capability. Future missions need to take into account the ongoing scientific need for all-sky X-ray monitoring.

## ACKNOWLEDGMENTS

SDV thanks the authors and journals who gave permission for their figures and portions of the captions to be reproduced here and Hale Bradt and the ASM team at MIT for providing statistics on ASM related publications. SDV was supported in part by NASA through Grant NAG5-6711.

## REFERENCES

- Chiang, J., Reynolds, C.S., Blaes, O.M., Nowak, M.A., Murray, N., Madejski, G., Harshill, H.L., & Magdziarz, P. 2000, *ApJ*, 528, 292.
- Choudnury, M., Rao, A.R., Vadawale, S.V., & Jain, A.K. 2003, *ApJ*, 593, 452.
- Clarkson, W.I., Charles, P.A., Coe, M.J. & Laycock, S. 2003a, *MNRAS*, 339, 447.
- Clarkson, W.I., Charles, P.A., Coe, M.J., Laycock, S., Tout, M.D. & Wilson, C.A. 2003b, *MNRAS*, 343, 1213.
- Grimm, H.-J., Gilfanov, M., & Sunyaev, R. 2002, *A&A*, 391, 923.
- Grimm, H.-J., Gilfanov, M., & Sunyaev, R. 2003, *MNRAS*, 339, 793.
- Katz, J. 1973, *Nature Physical Sciences*, 246, 87.
- Levine, A.M., Bradt, H., Cui, W., Jernigan, J.G., Morgan, E.H., Remillard, R., Shirey, R.E., & Smith, D.A. 1996, *ApJL*, 469, L39.
- Matilsky, T., Gursky, H., Kellogg, E., Tananbaum, H., Murray, S., & Giacconi, R. 1973, *ApJ*, 181, 753.
- McGowan, K.E., Priedhorsky, W.C., & Trudolyubov, S.P. 2003, *astro-ph* 0310425.
- Miller, J., & Garcia, M. 2002, editors, <http://asc.harvard.edu/xrbconf>.
- Ogilvie, G.I., Dubus, G. 2001, *MNRAS*, 320, 485.
- Paul, B., Kitamoto, S., & Makino, F. 2000, *ApJ*, 528, 410.
- Priedhorsky, W.C., Peele, A.g., & Nugent, K.A. 1996, *MNRAS*, 279, 733.
- Vrtilek, S.D., Raymond, J.C., Boroson, B., Kallman, T., Quaintrell, H., & McCray, R. 2001, *ApJL*, 563, 139L.
- Vrtilek, S.D., Raymond, J.C., Boroson, B., McCray, R., Smale, A., Kallman, T., & Nagase, F. 2003, *PASP*, 115, 1124.
- Wijers, R.A.M.J., & Pringle, J.E. 1999, *MNRAS*, 308, 207.
- Wojdowski, Patrick; Clark, George W.; Levine, Alan M.; Woo, Jonathan W.; Zhang, Shuang Nan 1998, *ApJ*, 502, 253.